

Wind power integration into the Northern Interconnected Power System of Chile

Dario Lafferte
University of Kassel
Department of Electric Power Supply Systems
Kassel, Germany
lafferte@student.uni-kassel.de

Abstract—This paper analyses the impact of wind power integration into the Northern Interconnected Power System of Chile (SING) on voltage stability, considering the Chilean conditions for wind power generation, such as the electricity market and its legal framework, wind potential studies for SING's areas, the grid code requirements, the structure of the power system and the negative effects of cosmic rays on power electronics, due to the significant altitudes of the selected wind locations for power generation. Doubly fed induction generators have been chosen according to its fault ride through capability and reduced semiconductor surface, minimizing the failure risk on power electronics. The crowbar protection has been improved to achieve the grid code requirements. Simulations are performed considering a high voltage transmission network model of SING during faults and at quick changes of loads and power generation. Moreover, the maximal feasible wind power feeding into SING had been also evaluated.

Keywords—wind power integration, doubly fed induction generators, grid code, fault ride through, voltage support, crowbar protection, longitudinal transmission networks.

I. INTRODUCTION

Wind power generation has been experiencing a rapid world development in the last decade with a cumulative market growth of more than 12.5%, representing a strong growth for a manufacturing industry given the current world economic situation [1]. Wind power also becomes important for the Chilean electricity market with an increasing number of projects [2], as a reaction to the legal reforms to promote the renewable energies for power generation and the energy crises of the last decade. Chile significantly lacks its own fossil resources and is highly dependent on imported energy sources, a situation which has led to regular power shortages in the past [3]. Chile was the world pioneer country that deregulated and privatized the electricity industry after the enactment of the Electricity Law in 1982 [4]. Therefore, the Chilean energy matrix is the result of the selection of low-cost energy sources due to the electricity market liberalisation, though the supply security was only ensured by signing reliable contracts and protocols and the needed technical measures were not realised, such as gas storage for the regulation of supply disruptions and the consideration of the current high energy costs [5]. The challenge for Chile is to achieve important energy security and to diversify the energy matrix through the procurement of its

own renewable energy resources and foreign credible and reliable energy suppliers [4,6,7].

The entire Chilean power system is divided in two interconnected power systems and two small grids because of the country's geography and the huge distances that cause different challenges for the grid voltage stability. The present work focuses on large wind power integration in the Northern Interconnected Power System of Chile (SING). SING is a strong predominant thermoelectric system (97.4% [8]), which corresponds to about 25% of the entire installed capacity of Chile and powers the cooper mining industry, which is fundamental for the Chilean economy. Furthermore, SING, such as the other Chilean grids, has a longitudinal structure with a negative impact on power system stability. Previous works focused on meshed power systems (such as in Europe), but this acquired knowledge from meshed networks cannot be directly applied to power systems with longitudinal structures, due to the fact that the effects of large scale wind power integration on system stability strongly depend on the characteristics of the transmission network [9]. Besides the network's structure, the best wind locations for power generation in SING are situated at considerable heights [10], increasing the failure rate of power electronics because of the negative influence of the cosmic rays on power electronic devices [11]. In addition, a deregulated generation market and the legal framework for the renewable energies require cost-efficient alternatives for power generation.

It is well known that a significant penetration of wind energy in power systems may cause significant problems to the power system stability due to the random nature of the wind and the characteristics of the wind energy converters (WEC). Large scale wind power connected into the transmission network (110 kV – 220 kV) will increase the difficulties in operation of the power system and can lead to problems of voltage stability, adding further challenges to the grid keeping the line voltage within a tolerance range. When wind parks are connected into the power system, faults can cause a voltage collapse due to the influence of induction machines; voltage stability deteriorates and network losses increase significantly [12,13]. Therefore, it is important to analyse the impact of wind power integration on voltage stability during faults for longitudinal networks, such as SING. The fault ride through requirements of the Chilean grid code for WEC, as the

European grid codes, demand voltage support and reactive power supply during and after faults [14], which means that the wind generators have to be connected through a back-to-back converter with the grid to provide reactive power support, without ignoring the negative cosmic rays influence on power electronics and the cost-efficient requirements of the electricity market for WEC.

Considering those conditions and restrictions, the wind power integration in Chile needs a power generation technology which is capable of riding through any system disturbances, supporting the grid voltage and supplying reactive power and also disposing of a limited semiconductor surface. Doubly fed induction generators (DFIG) meet the fault ride through requirements and the converter has to be designed for only 30% of the rated generator's capacity. The wind power integration into SING has been simulated considering a 120 MW DFIG-based wind park during faults and at quick changes of loads and power generation, according to the grid code requirements. Moreover, the maximal feasible wind power feeding into SING had been also evaluated.

II. CHILEAN CONDITIONS FOR WIND POWER INTEGRATION

A. The Chilean electricity market and its legal framework

Chile was the world pioneer country in deregulating and privatizing the electricity industry at the beginning of the eighties with the promulgation of the Electricity Law in 1982, restructuring the electricity market in three segments: generation, transmission and distribution. The generation is defined as a deregulated competitive market with freedom to invest, operating under a short run marginal cost pool-dispatch regime, while the transmission and the distribution are recognized and handled as natural monopolies with regulated tariffs. The main consequence for the generation is the fact that all generation technologies have to compete under equal opportunities. Expressed in another way, this scenario was adverse for the renewable energies, then they should compete with conventional power plants in a deregulated market with the same price and quality conditions, making the investments in this sector unattractive.

After the Argentina Gas Crisis and the consequent energy crisis in Chile in 2004, due to the fact that 94% of the gas consumption in the northern regions came from the SING's power demand [15], began a legal reform process with the enactment of many laws and decrees to promote the integration of renewable energies into the Chilean electricity market. The Chilean electricity law identifies Non-Conventional Renewable Energies (NCRE) as the generation from non-conventional sources connected to the grid, such as wind, geothermal, solar, biomass, cogeneration and small hydro generation up to 20 MW (to differentiate this from the large hydro generation). The reform's purpose was to procure favourable conditions and benefits for the use of NCRE by the Chilean government. Nevertheless, the reforms did not consider subsidies for the NCRE and intended only to create similar market conditions, such as e.g. the last Law 20,690 (2013), promoting the diversification of the energy matrix through the roll-out of NCRE with the aim to generate 20% of the country's demand using renewable sources by 2025. This scenario requires cost-

efficient NCRE alternatives to incentivize the investments in the generation sector.

B. Wind Potential of Chile

Several studies have been performed to determine the wind potential of Chile for power generation. The entire country has a gross wind potential of approximately 40-44 GW. Nevertheless, the exploitable wind potential in SING ranges to 1.5 GW according to [16]. The present work considers three wind locations for the integration analysis: *Calama Norte*, *Calama Oeste* and *Sierra Gorda*. These wind locations are situated near to important substations and mining consumptions and have excellent wind speed profiles. Fig. 1 shows a wind resource map with the three selected locations for wind power generation located in the most important cooper mining area of Chile [17].

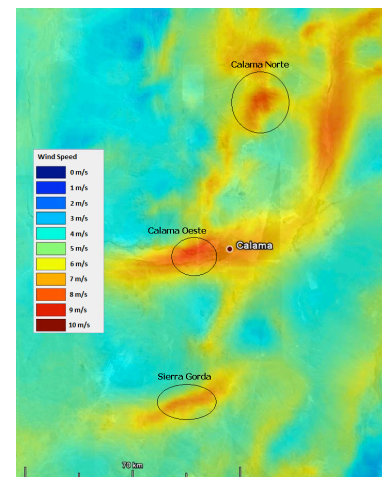


Fig. 1. Wind resource map of SING

C. The Northern Interconnected Power System

The Northern Interconnected Power System (SING) powers the northern Chilean regions and the cooper mining industry. The installed capacity of SING reaches 4.67 GW and corresponds to 24.5% of the entire installed capacity of Chile [18]. Although SING only supplies 6.36% of the population, the mining and industrial consumptions represent more than 90% of SING's power demand [16]. SING is a strong thermoelectric system (97.4%) and currently has four solar plants (23.5 MW) and one wind park (90 MW) connected to the grid. Nevertheless, until March 2014 these power plants have not been in commercial operation [18]. It should also be noted that the maximum power generation and the maximum power demand of SING in 2013 were 2.22 and 2.06 GW respectively [19]. This over-dimensioning in SING's generation could represent a technical and economic barrier for the wind power. However, the Economic Load Dispatch Centre of SING (CDEC-SING) restricts the operation of several power plants as a result of the deficiency in power reserve [16]. The development of wind power in recent years shows a world trend towards the grid integration of large wind parks to the high voltage (HV) levels. Therefore, SING has been modelled considering the HV levels (110 – 220 kV) of the transmission system and all necessary voltage levels to simulate the power

plants and loads. SING's model has been developed using the power system analysis software Digsilent PowerFactory. The single-line diagram of SING is shown in Fig. 2.

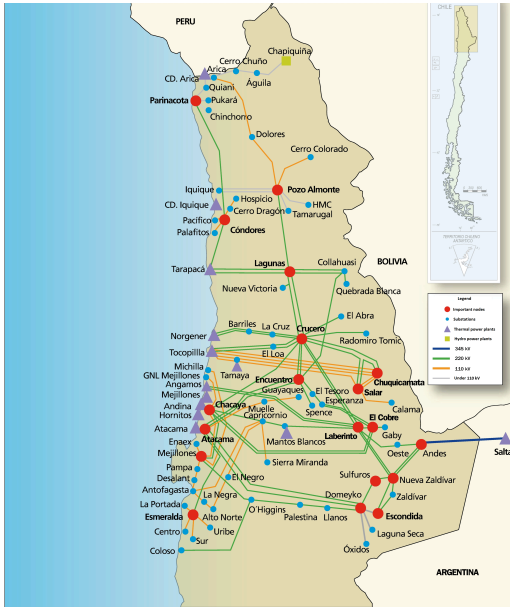


Fig. 2. Single-line diagram of SING (source: CDEC-SING)

D. Cosmic rays influence on SING's areas

The considered wind locations are situated on significant altitudes between 2,000 and 3,000 m.a.s.l. This situation increases the influence of cosmic rays on power electronics due to the fact that the cosmic radiation can induce substantial failure rates in high power devices [11]. The failure increment, also with a proper dimension, represents an important risk for the operational safety of long-term power electronics. An energy converter with a high power capacity implies a large semiconductor surface and finally an increase in the electronic failure rate. In addition, the Chilean grid code demands fault ride through capability for WEC connected to the grid. These requirements are often achieved by over-dimensioning the back-to-back converter, increasing the semiconductor surface. Consequently, a large semiconductor surface area means for long-term converters in power supply systems (with a minimum useful life of 20 years) a higher failure probability, increasing the maintenance and repair costs. Therefore, it is necessary to reduce the semiconductor surface in WEC to minimize the failure rate as well as the investment and maintenance costs. DFIG only need a back-to-back converter for 1/3 of the rated power and they fulfil the fault ride through requirements.

III. WIND POWER INTEGRATION

A. Voltage Stability

This work focuses on voltage stability for WEC connected to the grid under faults and at quick changes of consumptions and power generation, according to the fault ride through requirements for wind power. Reference [20] defines voltage

stability as the power system's ability to maintain the voltage level in all the busbars, under normal operating conditions as well as after perturbations. A power system enters a voltage instability state when a disturbance causes a progressive and uncontrollable voltage level degradation in a node, in an area or in the whole system. The main factor, which causes these unacceptable voltage profiles is the inability of the power system to meet the demand for reactive power, triggering voltage drops due to the changes in the power flows through the inductive elements of the transmission network. Therefore, considering the fault ride through requirements and the voltage stability problems under disturbances, this work concentrates on the short-term phenomenon. Short-term voltage stability involves system dynamics during the brief period after a major disturbance (several seconds) and its analysis requires the solution of appropriate system differential equations.

According to the grid code requirements, wind generators have to remain connected to the grid during and after faults, supporting the voltage and supplying reactive current. Therefore, this work analyses the transient response of wind parks connected to the grid under disturbances in consideration to the grid code conditions. The low voltage ride through requirements of the Chilean grid code are shown in Fig. 3 [21].

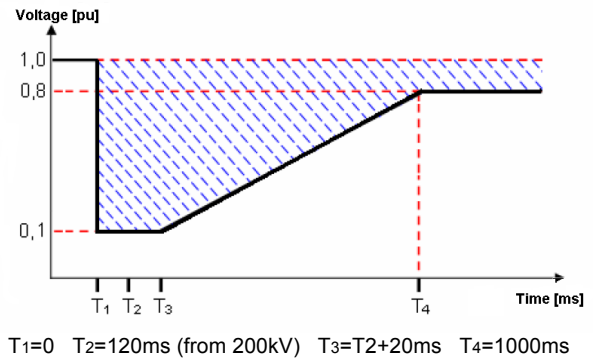


Fig. 3. Line-to-ground voltage requirements at the generator terminals

B. Doubly fed induction generators

Many authors have described the modelling of WEC with doubly fed induction generators (DFIG) [22-24]. Therefore, this work merely presents the main issues of DFIG. The typical configuration of DFIG-based WEC is shown in Fig. 4. This concept uses an induction generator whose stator windings are directly connected to the grid, while the rotor windings are connected to the network via a back-to-back PWM IGBT-based converter, linked through a DC bus. The DFIG configuration uses a wound-rotor induction generator with slip-rings to transmit current between the converter and the rotor winding and variable-speed operation is obtained by injecting a controllable voltage into the rotor at the desired slip frequency. The PWM converter allows variable speed operation of the wind turbine by decoupling the rotor mechanical speed from the synchronous grid frequency, thereby enabling DFIG under normal operation conditions to operate at optimal rotor speed thus maximizing the power generation. The back-to-back converter is composed of the rotor side converter (RSC) and the grid side converter (GSC), linked through a DC-link. The RSC regulates the active and reactive power injected by the

DFIG into the grid while the GSC regulates the DC-link voltage (keeping it constant at the pre-set value) and the power transit with the grid via the rotor.

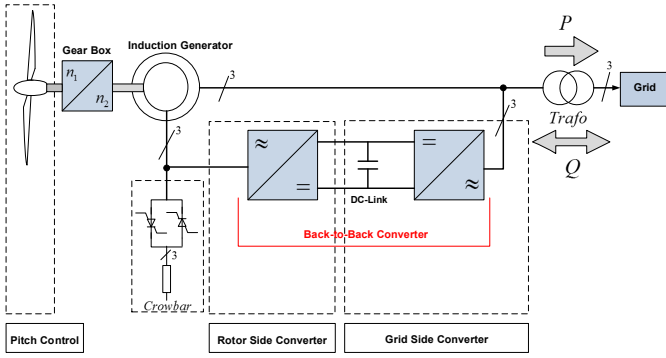


Fig. 4. DFIG-Based WEC System

The fact that the stator windings are connected directly to the grid makes the rotor windings susceptible to high currents induced during grid faults, which can damage the sensitive RSC. If the induced rotor voltage is higher than the DC-link voltage, the rotor currents are no longer controllable. The most common method to avoid high induced rotor currents during faults is the use of a crowbar protection system. While the crowbar is activated, DFIG behaves as a conventional squirrel cage induction generator with a higher rotor resistance expanding the critical rotor speed during the disconnection of the RSC from the rotor windings [25] and the generator control is lost and no grid support through the wind turbines is possible. Although the use of the crowbar system avoids the disconnection of DFIG-based WEC from the grid during faults, its use impedes the grid support. For that reason, the crowbar protection system has to be optimised by minimizing the bypass time in which the crowbar is activated and there is no reactive current supply to the grid. If the crowbar system only operates for several milliseconds (long enough to reduce the induced over-currents), it is possible to achieve a quasi-continuous reactive current support. The wind power integration analysis of this work considers the simulation of DFIG-based WEC with a minimized crowbar bypass time to achieve the Chilean fault ride through requirements for wind power plants.

C. Modeling of DFIG

The mathematical model of DFIG has been well documented in literature [22,24,26] and will only be discussed briefly here. Fig. 5 shows the equivalent circuit diagram of DFIG in which the RSC is integrated.

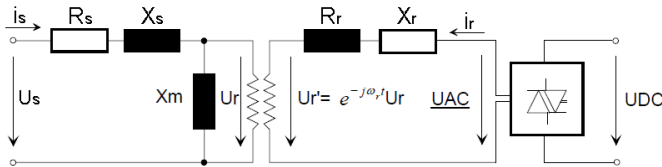


Fig. 5. DFIG equivalent circuit

The model equations for the voltage and flux linkage of the stator and rotor, with ω_{syn} rotating reference frame are derived as follows:

$$\underline{u}_s = R_s \underline{i}_s + \frac{1}{\omega_n} \cdot \frac{d\underline{\psi}_s}{dt} + j \frac{\omega_{syn}}{\omega_n} \underline{\psi}_s \quad (1)$$

$$\underline{u}_r = R_r \underline{i}_r + \frac{1}{\omega_n} \cdot \frac{d\underline{\psi}_r}{dt} + j \frac{\omega_{syn} - \omega_r}{\omega_n} \underline{\psi}_r \quad (2)$$

$$\underline{\psi}_s = (X_s + X_m) \underline{i}_s + X_m \underline{i}_r \quad (3)$$

$$\underline{\psi}_r = X_m \underline{i}_s + (X_m + X_r) \underline{i}_r \quad (4)$$

$$T_M - T_E = J \frac{d\omega_r}{dt} \quad (5)$$

where ω_{syn} is the synchronous speed, ω_n is the rated frequency of the grid and ω_r is the rotor angular speed. The RSC (shown in Fig. 5) is modelled by a fundamental frequency approach. The voltages of the AC and DC sides are related to each other by the modulation index PWM , which is defined in Cartesian co-ordinates by real (r) and imaginary (i) part:

$$U_{ACr} = \frac{\sqrt{3}}{2\sqrt{2}} \cdot PWM_r \cdot U_{DC} \quad (5)$$

$$U_{ACi} = \frac{\sqrt{3}}{2\sqrt{2}} \cdot PWM_i \cdot U_{DC} \quad (6)$$

Assuming a loss less PWM converter, we can find the expression for the AC and DC currents:

$$P_{AC} = \text{Re}(\underline{U}_{AC} \underline{I}_{AC}^*) = U_{DC} I_{DC} = P_{DC} \quad (6)$$

IV. DYNAMIC SIMULATIONS

To analyse the impact on voltage stability of wind power integration into SING under disturbances, a 120 MW DFIG-based wind park situated in *Calama Norte* was simulated, which is connected to the 220 kV substation of the open-pit cooper mine *El Abra* with a 23 km transmission line. The

dynamic simulations were performed in DlgSILENT *PowerFactory* 15.0 for the worst case scenario, i.e. under three phase short circuits, which cause the highest short circuit overcurrent and the deepest voltage dips [27]. The fault ride through response of WEC at the generator terminals was simulated under three phase short circuits at the wind park connection point (PCC) with the HV transmission network (220 kV). Fig. 6 shows the wind location *Calama Norte* and the section of the transmission network where it is situated.

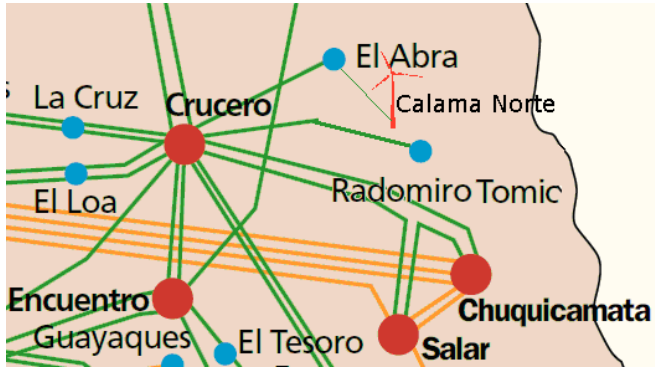


Fig. 6. Wind location *Calama Norte*

The crowbar bypass time was optimised as well to achieve the Chilean grid code requirements for wind power plants. The effects of load shedding or power plant outage on the wind park dynamic operation were also simulated. The wind park model for dynamic simulations is based on 2 MW DFIG-based generators. The output voltage of each DFIG is 0.69 kV working with a power factor of 0.95 according to the Chilean grid code. Each DFIG has a 0.69/20 kV transformer and the WEC are connected into SING through a substation, which elevates the line voltage from 20 up to 220 kV.

A. Three phase short circuit at the PCC

The dynamic response of WEC under three phase short circuits at PCC was simulated. The faults have a duration of 120 ms according to the fault clearance time of the grid code and the fault impedance is neglected [28]. Fig. 7 shows the line-to-ground voltage at the generator terminals. DFIG can ride through the three phase short circuit and the wind turbines remain connected to the grid. The line-to-ground voltage at the generator terminals achieve the fault ride through requirements and reactive power compensation is not necessary. DFIG recover the original operation point 30 ms after the fault clearance and the voltage stabilisation occurs through the activation of the pitch control. Fig. 8 shows the rotor current during the fault.

After the fault occurrence and once the rotor current exceeds the maximal rotor current value (1.9 p.u.), the crowbar protection is activated. The crowbar operation was optimised to reduce the dead time, in which DFIG cannot supply reactive power. 4 ms after the fault occurrence, the rotor current achieves the maximal allowed value and the crowbar will be activated. After 8 ms, the rotor current achieves the normal operation value and the crowbar will be disconnected and the RSC reconnected, supplying reactive current during the grid fault. The voltage response was also analysed in remote

busbars of the power system in order to consider the longitudinal structure of SING. Nevertheless, the line voltages of the analysed busbars meet the grid code requirements and the power system does not present voltage stability problems.

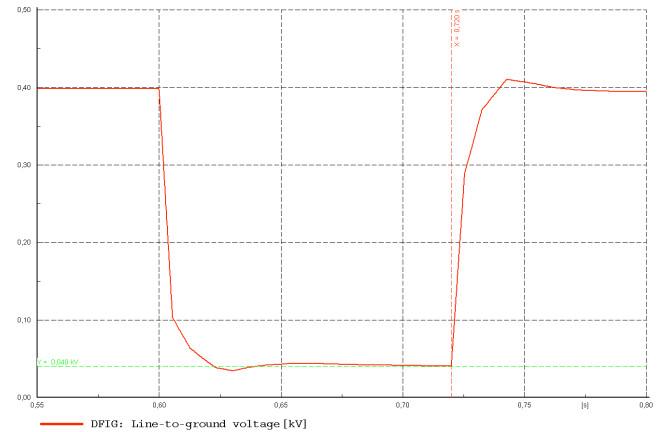


Fig. 7. Line-to-ground voltage at the generator terminals [kV]

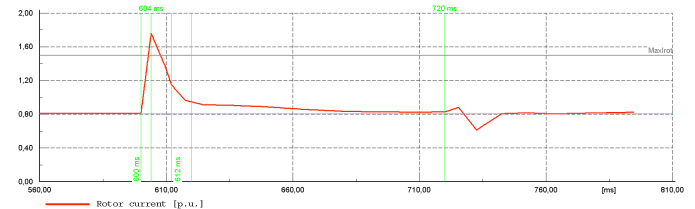


Fig. 8. Rotor current [p.u.]

B. Load shedding

Load shedding of important mining consumptions near to the wind park was simulated. The cooper mines *El Abra* and *Radomiro Tomic* were selected for the load shedding analysis (see Fig. 6), which represent a consumption of 91.28 and 103 MW respectively, both with a power factor of 0.98 [29]. Fig. 9 shows the temporal course of the load shedding and Fig. 10 shows the line voltage of the busbars *El Abra*, *Radomiro Tomic*, *Crucero* and the DFIG terminals. *Crucero* is the most important busbar system of the entire power system.

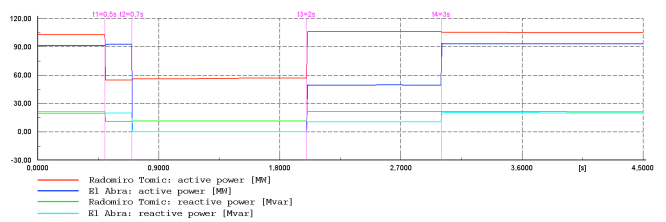


Fig. 9. Load shedding of *El Abra* and *Radomiro Tomic*

The loss of power consumption increases the busbar voltage, particularly near the load shedding. Even though the shown voltages (see Fig. 10) exceed the permitted voltage tolerance range, this occurs within the grid code allowed time. Fig. 11 shows the PV curves for the selected loads. A reduction of the active power lead to an increase of the voltage, as expected in transmission networks in normal operation. The load shedding does not activate the crowbar protection because the rotor current remains under the maximal value and the line

voltages of the selected loads achieve merely a voltage deviation of 2% around the set point 3 seconds after the normalization of the loads operation.

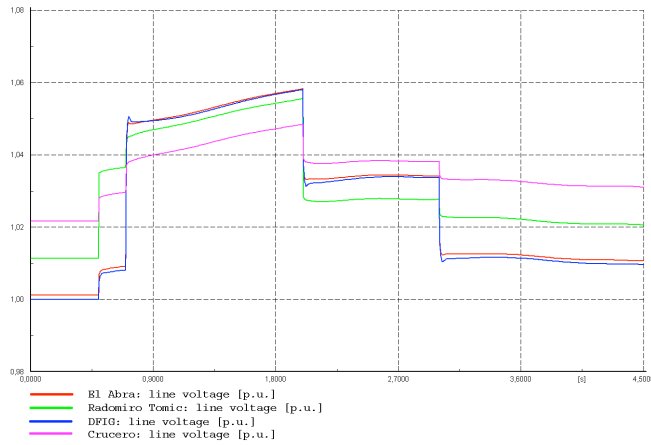


Fig. 10. Line voltages during the load shedding [p.u.]

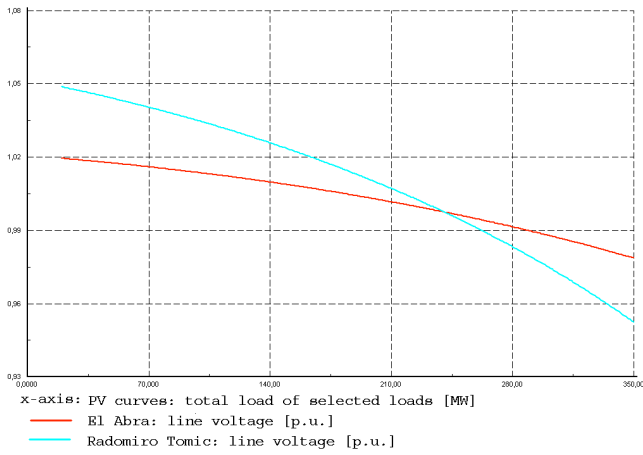


Fig. 11. PV curves for the selected loads

C. Disturbances at the Tocopilla Power Plant

Tocopilla is a thermoelectric power plant and is also the most important power plant of SING. *Tocopilla* has an installed nominal capacity of 1 GW with 10 generation units and powers approximately 25% of SING's entire power demand. However, by order of the CDEC-SING, the maximal power generation of *Tocopilla* cannot exceed 550-600 MW [30]. For the present analysis, three phase short circuits at the terminals of the generation unit U16 and a completely power plant outage of the generation unit U12 during the fault in unit U16 were simulated. The unit U16 has a nominal capacity of 400 MW with a maximal power generation of 130 MW and the unit U12 has a nominal capacity of 85.3 MW with a maximal power generation of 78.5 MW. The maximal power generation of each unit corresponds to SING's generation data of 2013. The power plant is connected to the *Crucero* substation and the cooper mine *Chuquicamata*, which is the largest open-pit cooper mine of the world. Fig. 12 shows voltage curves of important busbars of SING during the disturbance.

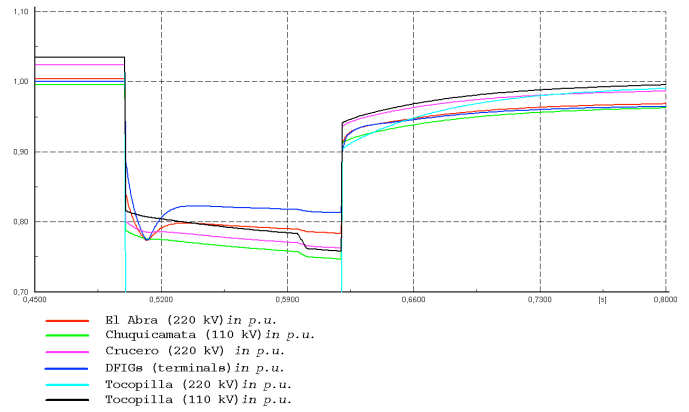


Fig. 12. Line voltages of important busbars

The busbar system for *Tocopilla* has two voltage levels; the unit U12 is connected to the 220 kV level and unit U16 is connected to the 110 kV level. The simulation shows the impact of the disturbance on busbar voltage, however, DFIG-based WEC ride through the fault, remaining connected to the grid, gives voltage support and achieves the grid code voltage requirements. Fig. 13 shows the rotor current of WEC. The induced over-current during the fault is not high enough to activate the crowbar protection. Moreover, the disturbance causes a reduction of the active power injection during the fault to approximately 50%, which is recovered after the fault clearance. Though it is a remote disturbance for the wind park, this is an important case because the system stability has been compromised.

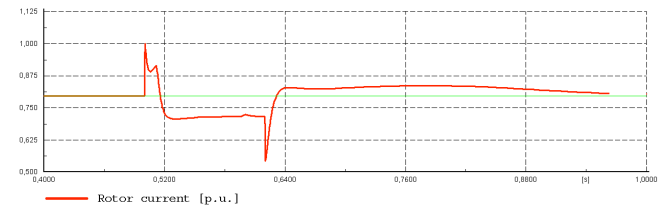


Fig. 13. Rotor current [p.u.]

D. Maximal power feeding for the selected wind locations

The selected wind locations for power generation are *Calama Norte*, *Calama Oeste* and *Sierra Gorda* (see Section II-B.). These wind locations dispose of a great wind potential and are situated near to important cooper mining consumptions. The distances between the wind locations and the transmission network, as well as SING's selected substations for wind power integration are shown in Table I. In order to evaluate the maximal power feeding for the selected wind locations, load flow calculations were used to analyse the loading capacity of the transmission lines between the selected substations and the rest of SING, considering the automatic tap adjustment of transformers and shut elements and the reactive power limits. The maximal acceptable loading capacity was set in 80-85%. Table II shows the maximal power feeding for each wind location without modifications of transmission lines.

TABLE I. DISTANCES BETWEEN WIND LOCATIONS AND SING

Location	Connection	Voltage Level	Distance
Calama Norte	El Abra	220 kV	23 km
Calama Oeste	Calama 110	110 kV	19 km
Sierra Gorda	El Tesoro	220 kV	5 km

TABLE II. MAXIMAL WIND POWER FEEDING WITHOUT MODIFICATION

Location	Connection	Maximal feeding	Affected power lines	Loading %
Calama Norte	El Abra	236 MW	Crucero-El Abra	81,8
Calama Oeste	Calama 110	78 MW	Salar-Calama	80,9
Sierra Gorda	El Tesoro	90 MW	Tesoro-Esperanza	81,6

The additional power injection from the wind parks was not considered in the design of the affected power lines and only these lines were overloaded. Therefore, the loading capacity of those lines was neglected to determine the maximal wind power feeding into SING. Table III shows the load flow calculation results with modification in the power capacity of the affected lines.

TABLE III. MAXIMAL WIND POWER FEEDING WITH MODIFICATION

Location	Connection	Maximal feeding	Affected power lines	Loading %
Calama Norte	El Abra	520 MW	Crucero-Encuentro #1	80,60
			Crucero-Lagunas #1	80,33
Calama Oeste	Calama 110	200 MW	Salar-KM6 #1	80,75
			Salar-KM6 #2	80,75
Sierra Gorda	El Tesoro	400 MW	El Cobre-Laberinto	80,27

If we consider that the maximal power generation for new power plants by order of CDEC-SING cannot exceed 400 MW, we therefore have a maximal wind power feeding into SING of 1 GW. The load flow calculations show a stable system with all busbar voltages within tolerances.

V. CONCLUSION

This work has shown that doubly fed induction generators are the best generation technology for wind power integration into SING according to the Chilean conditions, such as a deregulated electricity market and its legal framework, the wind potential in SING's areas, the SING's structure, the Chilean grid code requirements for fault ride through capability and the cosmic rays influence on selected wind locations. The Chilean electricity market and the respective legal framework require cost-efficient generation alternatives from non-conventional renewable energies given the absence of subsidies from the state, the significant lack of own fossil resources and the high dependency of imported energy sources, faced with the necessity of achieving a diversification of the energy matrix through its own renewable energy resources. Wind potential

studies have shown that important wind locations are situated on considerable altitudes increasing the negative influence of cosmic rays on power electronics. This situation restricts the use of WEC with full scale power converters due to the fact that a large semiconductor surface increases the failure risk of the electronic devices. Therefore, DFIG are the only alternative with a reduced semiconductor surface but capable to ride through any system disturbances and to provide reactive power support, according to the grid code requirements to incorporate wind power into SING.

Simulations have shown that the optimisation of the crowbar bypass time activation during grid faults is indispensable to achieve the fault ride through requirements of the Chilean grid code for wind power plants. During three phase short circuits near to the wind park, DFIG provide voltage support injecting reactive power and the crowbar activation avoids the disconnection of WEC from the grid. The wind power integration into SING was also simulated under load shedding of important cooper mining consumptions near to the wind park and the outage of the *Tocopilla* Power Plant. However, WEC remain connected to the grid providing voltage support. The maximal wind power feeding into SING for the selected wind locations was also considered and evaluated in approximately 1 GW.

REFERENCES

- [1] Global Wind Energy Council GWEC, "Global Wind Report – Annual market update 2013", April 2014. http://www.gwec.net/wp-content/uploads/2014/04/GWEC-Global-Wind-Report_9-April-2014.pdf
- [2] Centro de Energías Renovables (CER), CORFO, CDEC-SING, CDEC-SIC, "Estatus ERNC – Operación", report of the Centre for Renewable Energies of Chile, Santiago de Chile, 13/12/2013. http://cer.gob.cl/wp-content/uploads/downloads/2013/12/Estatus-General-Nov-_Operacion.pdf
- [3] M. Tokman, Chilean Energy Commission, "Política Energética: Nuevos Lineamientos – Transformando la crisis energética en una oportunidad", Comisión Nacional de Energía CNE, 2008. http://www.cne.cl/archivos_bajar/Politica_Energetica_Nuevos_Lineamientos_08.pdf
- [4] J. Aranceda, S. Mocarquer, R. Moreno, H. Rudnick, "Challenges on integrating renewables into the Chilean grid", POWERCON 2010, Hangzhou, China, October 2010.
- [5] Colegio de Ingenieros de Chile, "Plan estratégico país 2004 – 2010", Proyecto País del Colegio de Ingenieros de Chile, Santiago, Chile, 2004.
- [6] S. Mocarquer, "En la variedad está la energía, Pontificia Universidad Católica de Chile", Revista Universitaria, vol. 90, pp. 21-25, 2006.
- [7] H. Rudnick, "Seguridad energética en Chile: dilemas, oportunidades y peligros", Facultad de Ingeniería UC, Vicerrectoría de Comunicaciones y Asuntos Públicos, Pontificia Universidad Católica de Chile, Año 1, N° 4, November 2006.
- [8] Centro de Despacho Económico de Carga CDEC-SING, "Detalle anual de capacidad instalada por empresa - capacidad instalada por coordinado periodo 2004 – 2013", November 2013. http://cdec2.cdec-sing.cl/pls/portal/CDEC.MENU_INSTAL_GENE.show
- [9] C. Rahmann, „Auswirkungen von WEA-Einspeisung auf die Spannungsstabilität im chilenischen Übertragungsnetz“, PhD Thesis, Rheinisch-Westfälische Technische Hochschule Aachen, Klinkenberg publishers, 2010.
- [10] Ministerio de Energía de Chile, Departamento de Geografía de la Universidad de Chile, „Explorador de Energía Eólica – Información detallada sobre el recurso eólico disponible en Chile“, research project of the Chilean Ministry of Energy, the German Society of International

- Cooperation (GIZ) and the Department of Geography of the Universidad de Chile, Santiago de Chile, 2012.
<http://ernc.dgf.uchile.cl/Explorador/Eolico2/>
- [11] H. R. Zeller, "Cosmic ray induced failures in high power semiconductor devices, Microelectronics and Reliability", vol. 37, issues 10-11, pp. 1711-1718, October 1997.
- [12] I. Erlich, F. Shewarega, "Insert impact of large-scale wind power generation on the dynamic behaviour of interconnected systems", Bulk Power System Dynamics and Control – VII. Revitalizing Operational Reliability, 2007 iREP Symposium, pp. 1-7, 19-24, August 2007.
- [13] H. Shien, W. Weizhou, J. Huaisen, C. Gang, W. Fujun, L. Jun, "Integration of wind farm into Gansu power grid and its operation", International Conference on Sustainable Power Generation and Supply SUPERGEN '09, pp. 1-5, 6-7, April 2009.
- [14] Comisión Nacional de Energía de Chile (CNE), Norma técnica de seguridad y calidad de servicio (Chilean grid code), Santiago de Chile, August 2013.
- [15] C. Huneeus, "Argentina y Chile: el conflicto del gas, factores de política interna Argentina", Estudios Internacionales 158 – ISSN 0716-0240, Instituto de Estudios Internacionales, Universidad de Chile, 2007
- [16] GTD Ingenieros Consultores Ltda., "Análisis del impacto de centrales eólicas en el SING – Informe final", Proyecto Energías Renovables No Convencionales (MINENERGIA/GTZ), PN: 2007.2079.7, Feb. 2010.
- [17] Comisión Nacional der Energía de Chile (CNE), "Modelación del recurso solar y eólico en el norte de Chile", published by the Chilean Energy Commission, Santiago de Chile, May 2009.
- [18] Centro de Despacho Económico de Carga CDEC-SING, "Información técnica – Instalaciones de generación", technical report, March 2013.
http://cdec2.cdec-sing.cl/pls/portal/cdec.pck_inf_tec_nt_gene_pub.sp_centrales
- [19] Centro de Despacho Económico de Carga CDEC-SING, "Generación y demanda máxima anual del SING periodo 2004-2013", technical report, March 2013.
http://cdec2.cdec-sing.cl/pls/portal/cdec.pck_resumen_ejec_pub.rpt_gen_y_dda_max
- [20] P. Kundur, "Power system stability and control", EPRI Editors, McGraw-Hill, USA, 1994.
- [21] Comisión Nacional der Energía de Chile (CNE), Norma técnica de seguridad y calidad de servicio (Chilean grid code), Santiago de Chile, August 2013.
- [22] M. Pöller, "Doubly fed induction machine models for stability assessment of wind farms", in Proc. 2003 IEEE PowerTech Conference, Bologna, 2003.
- [23] V. Akhmatov, "Induction generators for wind power", Multi-Science Publishing Co. Ltd., UK, 2005.
- [24] G. Abad, J. López, M. Rodríguez, L. Marroyo, G. Iwanski, "Doubly fed induction machine – modeling and control for wind energy generation", IEEE Press, John Wiley & Sons, Inc., New Jersey, 2001.
- [25] A. P. Grilo, A. de Assis Mota, L. T. Moreira Mota, W. Freitas, "An analytical method for analysis of large-disturbance stability of induction generators", IEEE Trans. on Power Systems vol. 22, pp. 1861-1869, 2007.
- [26] C Hamon, K. Elkington, M. Ghandhari, "Doubly-fed induction generator modeling and control in DIGSILENT PowerFactory", POWERCON 2010 – International Conference on Power System Technology, pp. 1-7, Hangzhou, October 2010.
- [27] C. Rahmann, R. Palma-Behnke, "Optimal allocation of wind turbines by considering transmission security constraints and power stability", Energies Journal, pp. 294-311, Jan. 2013.
- [28] Dirección de Operación – Centro de Despacho Económico de Carga CDEC-SING, "Cálculo del nivel máximo de cortocircuito: Procedimiento", CDEC-SING P-0021/2010, Juni 2010.
- [29] Centro de Despacho Económico de Carga CDEC-SING, Datos de Operación del SING:
http://cdec2.cdec-sing.cl/pls/portal/cdec.pck_web_cdec_pages.pagina?p_id=1087
- [30] CDEC-SING, "Informe: Respuestas a observaciones recibidas al documento Estudio para plan de defensa contra contingencias extremas", technical report, 2008.